Diindenoperylene as ambipolar semiconductor: Influence of electrode materials and mobility asymmetry in organic field-effect transistors

Cite as: Appl. Phys. Lett. **98**, 233304 (2011); https://doi.org/10.1063/1.3598423
Submitted: 09 February 2011 . Accepted: 19 May 2011 . Published Online: 10 June 2011

Matthias Horlet, Michael Kraus, Wolfgang Brütting, and Andreas Opitz

Diindenoperylene as ambipolar semiconductor: Influence of electrode materials and mobility asymmetry in organic field-effect transistors

Matthias Horlet, Michael Kraus, Wolfgang Brütting, and Andreas Opitz[a)]
Institute of Physics, University of Augsburg, 86135 Augsburg, Germany

(Received 9 February 2011; accepted 19 May 2011; published online 10 June 2011)

Organic field-effect transistors were prepared using diindenoperylene as molecular semiconductor. An insulating alkane layer was used to separate the semiconductor from the underlying oxide and to suppress effects of electron traps at that surface. Diindenoperylene transistors were studied for various electrode materials. Unipolar p- and n-type as well as ambipolar devices were realized. An electron mobility of up to 0.14 $cm^2/V\,s$ and a hole mobility of up to 0.052 $cm^2/V\,s$ were found. The temperature dependent analysis shows similar trap distributions for both carrier types. Therefore the asymmetry in electron and hole transport seems to be an intrinsic effect of diindenoperylene. © *2011 American Institute of Physics*. [doi:10.1063/1.3598423]

The transport of electrons and holes in organic semiconductors can be realized by the reduction in bulk and interface trap states[1–3] as well as by adjustment of the injection barriers.[4] With these requirements bipolar transport has proven to be an intrinsic property of organic semiconductors as shown first for single crystals[5] and later on for thin films, especially in field-effect transistors.[3] Diindenoperylene[6] [DIP, $C_{32}H_{16}$—molecular structure shown in Fig. 1(a)] has been shown to exhibit electron and hole transport in single crystals. It is stable against oxidation[6] and decomposition even at elevated temperatures.[7] Due to the good crystallization behavior[8] DIP is a promising candidate for the application in field-effect transistors[9] and solar cells.[10] In this letter the ambipolar and bipolar transport is analyzed for DIP in thin-film transistors.

Thin-film transistors were prepared on highly doped silicon wafers with a 320 nm thermally grown oxide. Additionally a layer of the insulating long chain alkane tetratetracontane (TTC, $C_{44}H_{90}$) was deposited by thermal evaporation[11] (thickness about 10 nm) to separate the charge carrier transport in the molecular semiconductor from the silicon oxide surface. The excellent passivation behavior of TTC was reported in the literature.[12] TTC forms crystalline layers of upright standing, elongated molecules.[11] The layers were smoothed by thermal annealing at 60 °C for 2 h as shown earlier.[13] 25 nm of DIP—purified by thermal gradient vacuum sublimation—were deposited as active, semiconducting layer on top of a 10 nm thick TTC layer by thermal evaporation. The whole processing was carried out under high vacuum or under inert atmosphere. The morphology of such a film is shown by a scanning force microscopy image in Fig. 1(b). It is clearly visible that DIP forms a polycrystalline film with a typical grain diameter of about 250 nm. Larger grain size can be realized in DIP films by substrate heating during the evaporation of DIP.[14] This process, however, is not applicable here due to the low melting point of the TTC layer. Therefore the annealing temperature of the TTC layer is limited to 60 °C and the substrate temperature during evaporation of DIP is kept at room temperature. Various electrode materials (aluminum, silver, tetracyanoquinodimethane-tetrathiafulvalene TTF-TCNQ) have been used to realize unipolar electron, unipolar hole, and ambipolar transport in different transistors in a top contact geometry. The metal layers had a thickness of 50 nm and the organic metal TTF-TCNQ a thickness of 150 nm. Furthermore field-effect transistors (FETs) with two different electrode materials were prepared by a parallactic shadow mask displacement technique.[15] Thereby the Al layer was evaporated at first and afterwards with a slight lateral shift the TTF-TCNQ layer. The resulting transistor is displayed as cross section sketch in Fig. 1(c). The electrical characterization was performed under high vacuum conditions in a cryostat. The measured output characteristics at room temperature have been analyzed by the transfer length method[16] using channel lengths between 50 and 150 μm whereas the analysis in the linear range using the Shockley equation has been applied for the examination of temperature dependent measurements to determine the field-effect mobility. The variations in mobility between several produced devices with equivalent injection behavior were less than 10%. The two best samples are used to determine the here given averaged values.

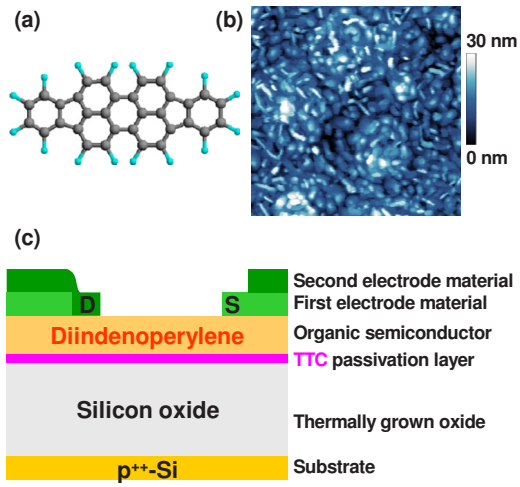

FIG. 1. (Color online) (a) Molecular structure of DIP (DIP, $C_{32}H_{16}$). (b) Scanning force microscopy image of a 25 nm DIP film on top of a 10 nm TTC layer. The image size is 2×2 μm^2. (c) Structure of the bottom-gate and top-contact field-effect transistor. Experiments are performed either with one single electrode material or with a bilayer of two different electrode materials.

[a)]Electronic mail: andreas.opitz@physik.uni-augsburg.de.

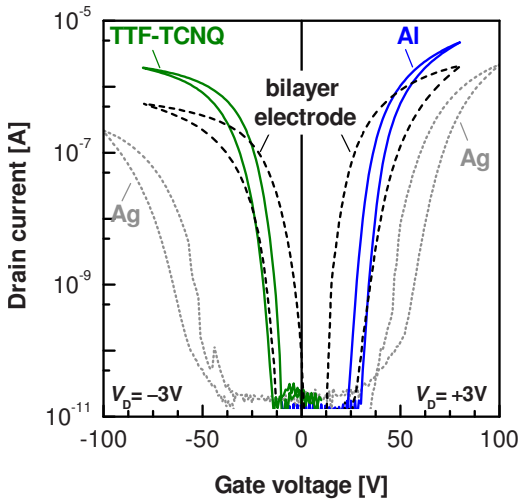

FIG. 2. (Color online) (a) Transfer characteristics in the linear range for different electrode materials (channel length 70 μm). The curves for the unipolar (ambipolar) devices are shown with solid, green and blue (dotted, gray) lines. The "bilayer electrode" device with Al and TTF-TCNQ as electrode materials has a channel length of 63 μm (dashed, black lines).

A set of transfer characteristics in the linear range for DIP FETs is displayed in Fig. 2. Unipolar electron transport is observed for Al electrodes and unipolar hole transport for TTF-TCNQ electrodes, respectively. Silver electrodes allow the injection of both electrons and holes into the channel, resulting in the shown ambipolar behavior. The mobilities determined by transfer length measurements are summarized in Table I. It was found that the values at room temperature for the different top contacts differ only by a factor of 2 with the electron mobility being 0.1 $cm^2/V\,s$ and the hole mobility up to 0.05 $cm^2/V\,s$. Remarkably, these mobilities obtained in thin-film transistors are one order of magnitude higher than the mobilities in DIP single crystals reported in the literature.[6,17] While in single crystals microcracks represent the major problem, in our thin film transistors the mobilities might be limited by the roughness of the underlying TTC film. The chosen film thickness is close to two complete monolayers of TTC. However, the TTC films show always steps with a height of 5 nm (the length of one molecule[11]). This roughness can cause electrostatic trapping and limit the mobilities.

The injection behavior for the different electrodes can be understood by comparison of the respective energy levels. The highest occupied molecular orbital (HOMO) and the transport gap of DIP are reported to be 5.35 eV (Ref. 10) and 2.7 eV,[18] respectively, resulting in a lowest unoccupied molecular orbital (LUMO) of 2.65 eV. As reported, e.g., for copper phthalocyanine,[19] the injection of electrons from Al top contacts (for work function values see Table I) works very well. A clear asymmetry between the injection barriers from the Fermi level of Al to the HOMO and LUMO of DIP is expected, thus no holes are injected from Al electrodes. There should also be an asymmetry for the corresponding injection barriers from Ag electrodes, however, in this case we can observe that both carrier types are injected. To explain the good injection behavior for electrons from Al into DIP and the reduced injection performance from Ag into the DIP LUMO a shift in the work function in the top contact geometry to lower values as the given numbers of free surfaces is needed. This can be possibly due to the lowering of the work function in contact with organic materials by the push-back effect.[20] Additional effects (like penetration of metal atoms[21] or damaging of molecules[22]) can appear due to the evaporation of the metal on top of the semiconductor resulting in the observed injection behavior. Different values of the work function of TTF-TCNQ are reported in the literature[23,24] with the lower limit being comparable to clean Ag surfaces. Nevertheless, the injection of holes into DIP is favored from the one-dimensional organic metal. In the results presented here the good alignment of the work functions of Al and TTF-TCNQ electrodes to the respective transport levels in DIP can be seen in the strongly reduced contact resistances (by a factor of 10 in comparison to the Ag electrode).

Additionally, drastically reduced switch-on voltages are observed for the unipolar transistors in comparison to the ambipolar ones. This effect can be explained by the better alignment of the contact Fermi level to the respective quasi-Fermi levels of the organic semiconductor in the unipolar case in contrast to the ambipolar case. These reduced switch-on voltages, resulting also in reduced threshold voltages, are the reason for the higher currents in the unipolar FETs having the same mobility as the ambipolar device with Ag electrodes. The effect of two different electrodes giving a good unipolar injection is transferred to an ambipolar field-effect transistor with "bilayer electrodes" as sketched in Fig. 1(c). As can be seen also in Fig. 2 the low switch-on voltages can be reproduced. However, lower mobilities are observed for the FETs with combined Al/TTF-TCNQ electrodes. The determination of the channel length is inaccurate in the device with two electrode materials so that the same values for the contact resistances are used as for the unipolar devices. However, the differences in the mobilities due to the fixed contact resistances are negligible. In addition, using different materials for source and drain contacts causes a built-in potential for the drain current which is not considered in the analysis.

A temperature dependent measurement has been performed for a device with the combined Al and TTF-TCNQ electrodes. The mobilities determined from the linear regime without consideration of the contact resistances are shown in Fig. 3 as a function of temperature. The electron mobility is always higher than the hole mobility, even though the asymmetry between electron and hole transport in this case is smaller than shown in Table I. Thereby a decreasing slope in the diagram—logarithm of the mobility versus reciprocal temperature—for lower temperature is observed resulting in

TABLE I. Averaged field-effect mobilities μ and contact resistances R_C for electron and hole transport at room temperature determined by the transfer length method for the different electrode materials together with their work functions Φ (in eV, see Refs. 19, 22, and 23). Additionally the ambipolar mobilities at room temperature determined from time-of-flight measurements on single crystals are given for comparison (see Ref. 6).

Electrode		Electron		Hole	
Material	Φ (eV)	μ_e ($cm^2/V\,s$)	$R_{C,e}$ (MΩ)	μ_h ($cm^2/V\,s$)	$R_{C,h}$ (MΩ)
Aluminum	3.6	1×10^{-1}	0.1	—	—
Silver	4.9	1×10^{-1}	1	2×10^{-2}	10
TTF-TCNQ	4.7–5.6	—	—	5×10^{-2}	1
Al/TTF-TCNQ		3×10^{-2}	0.1	7×10^{-3}	1
Single crystal		2×10^{-2}		3×10^{-3}	

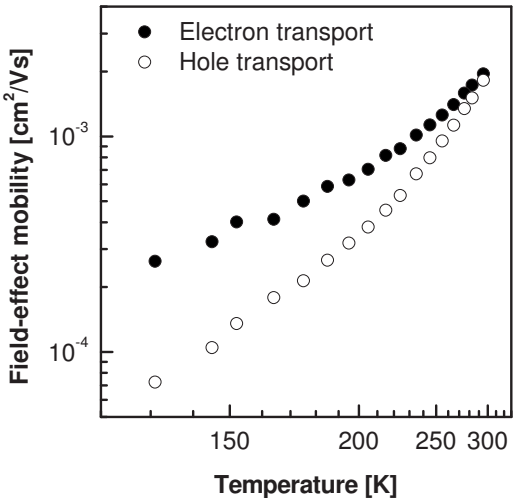

FIG. 3. Temperature dependent field-effect mobilities of electron and hole transport calculated from the linear range.

a lower activation energy at low temperatures. The fitted activation energy is reduced for the electron (hole) transport from 72 meV (105 meV) at room temperature to 28 meV (49 meV) in the low temperature range with an uncertainty of less than 3 meV. This observation is not describable with a pure activation behavior, a grain boundary behavior,[25] or grain boundary traps.[26] Therefore the analysis for trap states by Lang and co-workers was used.[27] The main feature here is the application of the same analysis technique for electron and hole transport measured on the same FET. In the analyzed range the density of states N can be fitted using an exponential distribution

$$N = N_0 \exp\left[-\frac{E}{E_0}\right], \tag{1}$$

where N_0 is the prefactor and E_0 the width of the distribution.

The distributions determined are very narrow, which is typical for the trap states in polycrystalline materials.[28] The resulting energetic width (prefactor) is about 23 meV (5×10^{21} eV^{-1} cm^{-3}) for electrons and about 20 meV (4×10^{21} eV^{-1} cm^{-3}) for holes. These very similar values for electrons and holes show that the asymmetry between electron and hole transport is not related to different trap densities like in CuPc.[13] It rather seems to be an intrinsic material property, e.g., the different π-orbital overlap between neighboring molecules in the HOMO and LUMO, respectively.[29] Another possibility is a difference in tunneling barrier at the grain boundaries because electrons have to tunnel between the LUMO levels and the holes between the HOMO levels.

In conclusion, the bipolar nature of DIP was confirmed in FETs. The mobilities for electrons and holes are higher than the reported single crystal values.[6] However, the asymmetry between electron and hole transport has the same tendency to a higher electron mobility as in single crystals measured by time-of-flight technique. The asymmetry is based on intrinsic molecular properties because the determined density of states is very similar and equal transport state distributions are observed. The combination of two different electrode materials allows a high current also in the saturation regime[30] where the observation of light emission should be possible.

This work was supported by the Deutsche Forschungsgemeinschaft (DFG) within priority program Grant No. SPP1355 (Br 1728/8).

[1]K. H. Probst and N. Karl, Phys. Stat. Solidi A **27**, 499 (1975).
[2]J. Pflaum, J. Niemax, and A. Tripathi, Chem. Phys. **325**, 152 (2006).
[3]L. L. Chua, J. Zaumseil, J. F. Chang, E. C. W. Ou, P. K. H. Ho, H. Sirringhaus, and R. H. Friend, Nature (London) **434**, 194 (2005).
[4]T. Yasuda, T. Goto, K. Fujita, and T. Tsutsui, Appl. Phys. Lett. **85**, 2098 (2004).
[5]N. Karl, *Landolt-Börnstein, New Series*, Vol. 41E, edited by O. Madelung, M. Schulz, and H. Weiss, , (Springer, Berlin, 2000).
[6]A. K. Tripathi and J. Pflaum, Appl. Phys. Lett. **89**, 082103 (2006).
[7]S. Sellner, A. Gerlach, F. Schreiber, M. Kelsch, N. Kasper, H. Dosch, S. Meyer, J. Pflaum, M. Fischer, and B. Gompf, Adv. Mater. (Weinheim, Ger.) **16**, 1750 (2004).
[8]A. C. Dürr, F. Schreiber, M. Münch, N. Karl, B. Krause, V. Kruppa, and H. Dosch, Appl. Phys. Lett. **81**, 2276 (2002).
[9]N. Karl, Synth. Met. **133–134**, 649 (2003).
[10]J. Wagner, M. Gruber, A. Hinderhofer, A. Wilke, B. Bröker, J. Frisch, P. Amsalem, A. Vollmer, A. Opitz, N. Koch, F. Schreiber, and W. Brütting, Adv. Funct. Mater. **20**, 4295 (2010).
[11]M. Kraus, S. Richler, A. Opitz, W. Brütting, S. Haas, T. Hasegawa, A. Hinderhofer, and F. Schreiber, J. Appl. Phys. **107**, 094503 (2010).
[12]S. Ogawa, Y. Kimura, M. Niwano, and H. Ishii, Appl. Phys. Lett. **90**, 033504 (2007).
[13]M. Kraus, S. Haug, W. Brütting, and A. Opitz, Org. Electron. **12**, 731 (2011).
[14]M. Münch, Ph.D. thesis, University of Stuttgart, 2001.
[15]R. Schmechel, M. Ahles, and H. von Seggern, J. Appl. Phys. **98**, 084511 (2005).
[16]S. Luan and G. W. Neudeck, J. Appl. Phys. **72**, 766 (1992).
[17]The low mobilities in the DIP single crystal are probably related to a structural phase transition occurring during cool down after the high temperature growth process. This phase transition generates internal stress which is released via the formation of small crystalline domains, Ref. 6.
[18]S. Krause, Ph.D. thesis, University of Würzburg, 2009.
[19]A. Opitz, M. Kraus, M. Bronner, J. Wagner, and W. Brütting, New J. Phys. **10**, 065006 (2008).
[20]N. Koch, J. Phys.: Condens. Matter **20**, 184008 (2008).
[21]A. C. Dürr, F. Schreiber, M. Kelsch, H. Carstanjen, and H. Dosch, Adv. Mater. (Weinheim, Ger.) **14**, 961 (2002).
[22]J. G. Xue, B. P. Rand, S. Uchida, and S. R. Forrest, J. Appl. Phys. **98**, 124903 (2005).
[23]K. Shibata, H. Wada, K. Ishikawa, H. Takezoe, and T. Mori, Appl. Phys. Lett. **90**, 193509 (2007).
[24]W. D. Grobman, R. A. Pollak, D. E. Eastman, E. T. Maas, and B. A. Scott, Phys. Rev. Lett. **32**, 534 (1974).
[25]G. Horowitz, R. Hajlaoui, D. Fichou, and A. El Kassmi, J. Appl. Phys. **85**, 3202 (1999).
[26]J. Levinson, F. R. Shepherd, P. J. Scanlon, W. D. Westwood, G. Este, and M. Rider, J. Appl. Phys. **53**, 1193 (1982).
[27]D. V. Lang, X. Chi, T. Siegrist, A. M. Sergent, and A. P. Ramirez, Phys. Rev. Lett. **93**, 086802 (2004).
[28]W. L. Kalb and B. Batlogg, Phys. Rev. B **81**, 035327 (2010).
[29]C. Schuster, M. Kraus, A. Opitz, W. Brütting, and U. Eckern, Eur. Phys. J. Spec. Top. **180**, 117 (2009).
[30]M. C. Gwinner, Y. Vaynzof, K. K. Banger, P. K. H. Ho, R. H. Friend, and H. Sirringhaus, Adv. Funct. Mater. **20**, 3457 (2010).